

Pion-induced K^* production with Σ^* baryon off proton target

Jie Xiang¹, Xiao-Yun Wang^{1,2}, Hao Xu³ and Jun He⁴

¹Lanzhou University of Technology, Lanzhou 730050, China

²Department of Physics, Lanzhou University of Technology, Lanzhou 730050, China

³Department of Applied Physics, School of Science, Northwestern Polytechnical University, Xi'an 710129, China

⁴Department of Physics and Institute of Theoretical Physics, Nanjing Normal University, Nanjing, Jiangsu 210097, China

E-mail: xywang@lut.edu.cn and junhe@njnu.edu.cn

Received 18 June 2020, revised 27 August 2020

Accepted for publication 27 August 2020

Published 27 October 2020



CrossMark

Abstract

In this work, the reaction $\pi^-p \rightarrow K^*\Sigma^*$ is investigated with an effective Lagrangian approach. The contributions from the Born terms, including the s , t , and u channel, are considered, and the Regge model and the Feynman model are applied to treat the t -channel contribution. The existing experimental data can be reproduced with the best-fitted χ^2 being 2.38 and 1.54 for the Feynman and Regge models, respectively. Moreover, it is found that the contribution from the t channel is dominant in the cross-section. The contribution of the u channel is mainly distributed at backward angles, and the contribution from the s channel is small and negligible. In the Feynman model, the contribution of the t -channel K exchange is much larger than the contribution of the K^* exchange, while in the Regge model the contribution of the t -channel K exchange is comparable to that of the K^* exchange. Prediction about the differential cross-section of the $\pi^-p \rightarrow K^*\Sigma^*$ reaction is also presented, which is helpful for clarifying the role of the Regge treatment. The current results suggest high-precision experimental measurements which can be performed at J-PARC and COMPASS.

Keywords: effective Lagrangian approach, Regge model, hadron states

(Some figures may appear in colour only in the online journal)

1. Introduction

Considering that the nucleon is the most popular hadron and the cornerstone of the observable world, the study of the nucleon and its resonance is an important topic in hadron physics. The nucleon resonance is composed of three quarks, the sum of which mass is much smaller than the total mass of a nucleon. Hence, spectroscopy of nucleon resonance is very important in understanding how quarks combine to form a hadron. Although many efforts have been made to understand the internal structure of nucleon resonances in the past, many puzzles in this research area still exist, such as the well-known 'missing resonance' problem [1, 2]. The nucleon resonance is usually studied in the meson production off a nucleon, especially a proton target. The pion-induced production process is an important route to nucleon resonance in history, and

the high-precision pion beams will be available in many large facilities, such as J-PARC and COMPASS [3, 4].

In the conventional constituent quark model, the nucleon resonance is composed of the three u/d quarks. In the early days, most of the nucleon resonances were observed in the pion-nucleon scattering [1]. In such a process, only the u/d quarks are involved, which leads to large production possibility of the nucleon resonances. However, to carry out further study of the internal structure of the nucleon resonances, the pion-induced strange production, where a strange quark pair is created, has special advantages. In such a process, the nucleon resonances can be further distinguished compared with the pion-nucleon scattering [5, 6].

In recent years, the strange component in nucleon resonances has attracted much interest in the community. It is suggested that a considerable hidden strange pentaquark

component exists in the nucleon, which is important in understanding the properties of a nucleon [7]. Such a picture was also applied to understand the issues in the nucleon resonances, such as the reverse mass order problem for the $\Lambda(1405)$ and $N(1535)$ [8]. It was further extended to the hidden-charm sector to predict the hidden-charm pentaquarks [9–11], which was confirmed by the LHCb Collaboration [12, 13]. Such experimental confirmations of the hidden-charm pentaquark give us more confidence about the hidden strange components in the nucleon resonances [14]. The pion-induced production of the hidden-charm/bottom pentaquarks were also predicted in the literature [15, 16].

To detect the hidden strange components in the nucleon resonance, a natural choice is the strange meson production process. In such a process, the strange quarks in the final state are from the hidden strange components in the nucleon resonance. In [17–23], the $\Lambda(1520)$ and $\Sigma(1385)$ photoproduction with a kaon meson was studied and the results indicate the states $N(2100)$ and $N(1875)$ may be candidates of the hidden strange molecular states [24]. Hence, the strange meson production will be more important in the future study of nucleon resonance.

In the literature, many strange meson photoproductions have been studied, such as with the final states $K^*\Lambda$ [25–29], $K\Sigma^*$ [22, 30], $K\Lambda(1520)$ [17, 19, 23, 31, 32], and ΞKK [33]. Some of the pion- or kaon-induced strange production can also be found in the literature [34–40]. However, the study of the process $\pi^-p \rightarrow K^*\Sigma^*$ is scarce, which we focus on in this work. Moreover, considering that the total spin of $K^*\Sigma^*$ is different from the total spin of $K\Sigma^*$, the two scattering processes of $\pi^-p \rightarrow K\Sigma^*$ and $\pi^-p \rightarrow K^*\Sigma^*$ may have their own advantages when studying strange baryons with different spin quantum numbers. For example, for nucleons with a spin-parity of $1/2^-$, it seems more advantageous to study them through the $\pi^-p \rightarrow K^*\Sigma^*$ reaction process. Fortunately, some experimental data on the $\pi^-p \rightarrow K^*\Sigma^*$ reaction exists [41–45]. Based on those data, we conduct a preliminary analysis of this reaction in this work, which may provide some valuable references for the experimental and theoretical research into the hidden strange pentaquark.

This paper is organized as follows. After an introduction, the formalism for the calculation is presented. The numerical result and discussion are given in section 3. Finally, this paper ends with a brief conclusion.

2. Formalism

The basic tree level Feynman diagrams of the $\pi^-p \rightarrow K^*\Sigma^*$ reaction are illustrated in figure 1. These include s -channel nucleon exchanges, t -channel K/K^* meson exchange, and the u channel with an intermediate Σ baryon.

2.1. Lagrangians and amplitudes

To gauge the pion-induced production of $K^*\Sigma^*$, the relevant Lagrangian densities are required, which have been used in [21, 28, 30, 37, 46]. Wherein, the Lagrangians corresponding

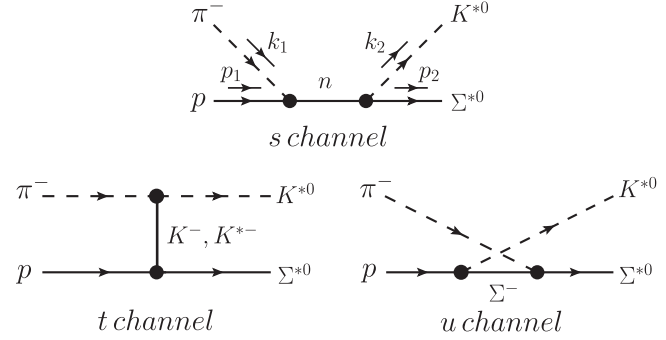


Figure 1. Feynman diagrams for the $\pi^-p \rightarrow K^*\Sigma^*$ reaction.

to the s channel are written as

$$\begin{aligned} \mathcal{L}_{K^*N\Sigma^*} = & -i \frac{f_{K^*N\Sigma^*}^{(1)}}{m_{K^*}} \bar{K}_{\mu\nu}^* \Sigma^{*\mu} \cdot \tau \gamma^\nu \gamma_5 N \\ & - \frac{f_{K^*N\Sigma^*}^{(2)}}{m_{K^*}} \bar{K}_{\mu\nu}^* \Sigma^{*\mu} \cdot \tau \gamma_5 \partial^\nu N \\ & - \frac{f_{K^*N\Sigma^*}^{(3)}}{m_{K^*}} \partial^\nu \bar{K}_{\mu\nu}^* \Sigma^{*\mu} \cdot \tau \gamma_5 N + \text{H.c.}, \end{aligned} \quad (1)$$

$$\mathcal{L}_{\pi NN} = -ig_{\pi NN} \bar{N} \gamma_5 \vec{\tau} \cdot \vec{\pi} N, \quad (2)$$

for the t channel:

$$\begin{aligned} \mathcal{L}_{K^*K\pi} = & g_{K^*K\pi} [\bar{K} (\partial^\mu \vec{\tau} \cdot \vec{\pi}) - (\partial^\mu \bar{K}) \vec{\tau} \cdot \vec{\pi}] K_\mu^* \\ & + \text{H.c.}, \end{aligned} \quad (3)$$

$$\mathcal{L}_{\pi K^*K^*} = g_{\pi K^*K^*} \varepsilon^{\mu\nu\alpha\beta} \partial_\mu \bar{K}_\nu^* \vec{\tau} \cdot \vec{\pi} \partial_\alpha K_\beta^*, \quad (4)$$

$$\mathcal{L}_{KN\Sigma^*} = \frac{f_{KN\Sigma^*}}{m_K} \bar{N} \Sigma^{*\mu} \cdot \vec{\tau} (\partial_\mu K) + \text{H.c.}, \quad (5)$$

for the u channel:

$$\begin{aligned} \mathcal{L}_{K^*N\Sigma} = & -g_{K^*N\Sigma} \bar{N} \Sigma \left(K^* - \frac{\kappa_{K^*N\Sigma}}{2m_N} \sigma_{\mu\nu} \partial^\nu K^{*\mu} \right) \\ & + \text{H.c.}, \end{aligned} \quad (6)$$

$$\mathcal{L}_{\Sigma^*\pi\Sigma} = \frac{g_{\Sigma^*\pi\Sigma}}{m_\pi} \bar{\Sigma}^{*\mu} (\partial_\mu \vec{\tau} \cdot \vec{\pi}) \Sigma + \text{H.c.}, \quad (7)$$

where $K_{\mu\nu}^* = \partial_\mu K_\nu^* - \partial_\nu K_\mu^*$. The N , K^* , Σ^* , π , K , and Σ are the nucleon, $K^*(890)$, $\Sigma^*(1385)$, π , K meson, and Σ baryon field, respectively. The $\vec{\tau}$ is the Pauli matrix.

For the πNN interaction vertex, we adopt $g_{\pi NN}^2/4\pi$ as 12.96 [47]. In addition, we take the following coupling constant values [28, 37, 46, 48], i.e. $g_{K^*N\Sigma} = -2.46$, $\kappa_{K^*N\Sigma} = -0.47$, $g_{\pi K^*K^*} = 7.45 \text{ GeV}^{-1}$. In addition, the coupling $f_{K^*N\Sigma^*}^{(1)}$ can be obtained from SU(3) flavor symmetry relations, which gives $f_{K^*N\Sigma^*}^{(1)} = -2.6$ [49]. In this work, we take $f_{K^*N\Sigma^*}^{(2)} = f_{K^*N\Sigma^*}^{(3)} = 0$ because of a lack of relevant information [49].

Moreover, the coupling constants $g_{K^*K\pi}$, $g_{\Sigma^*\pi\Sigma}$ can be determined from the decay widths of the $\Gamma_{K^* \rightarrow K\pi}$ and $\Gamma_{\Sigma^* \rightarrow \pi\Sigma}$, respectively, as

$$\Gamma_{K^* \rightarrow K\pi} = \frac{g_{K^*K\pi}^2 |\vec{p}_\pi^{\text{c.m.}}|^3}{2\pi m_{K^*}^2}, \quad (8)$$

$$\Gamma_{\Sigma^* \rightarrow \pi \Sigma} = \frac{f_1 g_{\Sigma^* \pi \Sigma}^2 |\vec{p}_{\Sigma}^{\text{c.m.}}|^3 (E_{\Sigma} + m_{\Sigma})}{12\pi m_{\pi}^2 M_{\Sigma^*}}, \quad (9)$$

with

$$E_{\Sigma} = \frac{M_{\Sigma^*}^2 + m_{\Sigma}^2 - m_{\pi}^2}{2M_{\Sigma^*}},$$

$$|\vec{p}_{\Sigma}^{\text{c.m.}}|^3 = \sqrt{E_{\Sigma}^2 - m_{\Sigma}^2},$$

$$|\vec{p}_{\pi}^{\text{c.m.}}|^3 = \frac{\sqrt{[m_{K^*}^2 - (m_K + m_{\pi})^2][m_{K^*}^2 - (m_K - m_{\pi})^2]}}{2m_{K^*}},$$

where the isospin factor f_1 for $\Sigma^* \rightarrow \pi \Sigma$ is 2. By taking the experimental data of the relevant particles in the PDG book [1], the coupling constants of $g_{K^* K \pi}$ and $g_{\Sigma^* \pi \Sigma}$ can be calculated. With mass $m_{K^*} = 891.7$ MeV and $M_{\Sigma^*} = 1383.7$ MeV, the total decay widths can be obtained as $\Gamma_{K^*} = 50.8$ MeV and $\Gamma_{\Sigma^*} = 36.0$ MeV. And with the branching ratio ($Br[K^* \rightarrow K\pi] = 1.00$, $Br[\Sigma^* \rightarrow \pi \Sigma] = 0.117$), we obtain $g_{K^* K \pi} = 3.26$ and $g_{\Sigma^* \pi \Sigma} = 0.68$.

To consider the size of the hadron, for the s and u channels with intermediate baryons, the form factors are adopted in our calculation as follows [21, 28, 46, 47, 50],

$$\mathcal{F}_{s/u}(q_{\text{ex}}) = \frac{\Lambda_{s/u}^4}{\Lambda_{s/u}^4 + (q_{\text{ex}}^2 - m_{\text{ex}}^2)^2}, \quad (10)$$

where q_{ex} and m_{ex} are the four-momentum and mass of the exchanged hadron, respectively. To reduce the free parameters, one takes $\Lambda_s = \Lambda_u$. For the t -channel K/K^* meson exchange [47], the form factor $\mathcal{F}_t(q_V)$ consisting of $\mathcal{F}_{K^* V \pi} = (\Lambda_t^2 - m_V^2)/(\Lambda_t^2 - q_V^2)$ and $\mathcal{F}_{V B B} = (\Lambda_t^2 - m_V^2)/(\Lambda_t^2 - q_V^2)$ are adopted with q_V and m_V being the four-momentum and mass of the exchanged meson, respectively. The values of the cutoffs Λ will be determined by fitting the experimental data.

According to the above Lagrangians, the scattering amplitude of the reaction $\pi^- p \rightarrow K^* \Sigma^*$ reads as

$$-i\mathcal{M}_i = \epsilon_{\mu}(k_2) \bar{u}_{\nu}(p_2) \mathcal{A}_i^{\mu\nu} u(p_1), \quad (11)$$

where ϵ_{μ} is the polarization vector of the K^* meson, and \bar{u}_{ν} and u are dimensionless Rarita–Schwinger and Dirac spinors, respectively.

The reduced amplitudes $\mathcal{A}_i^{\mu\nu}$ for s , t , and u channel contributions read as

$$\mathcal{A}_{s,(N)}^{\mu\nu} = i\sqrt{2} g_{\pi NN} \frac{f_{K^* N \Sigma^*}^{(1)}}{m_{K^*}} \mathcal{F}_s(q_{\text{ex}}) \gamma_{\sigma} \gamma^5$$

$$(k_2^{\nu} g^{\mu\sigma} - k_2^{\sigma} g^{\mu\nu}) \frac{(q_N + m_N)}{s - m_N^2} \gamma_5, \quad (12)$$

$$\mathcal{A}_{t,(K)}^{\mu\nu} = \sqrt{2} g_{K^* K \pi} \frac{f_{K N \Sigma^*}}{m_K} \mathcal{F}_t(q_V) \frac{1}{t - m_K^2}$$

$$(k_1 - k_2)^{\nu} [k_1^{\mu} + (k_1 - k_2)^{\mu}], \quad (13)$$

$$\mathcal{A}_{t,(K^*)}^{\mu\nu} = \sqrt{2} g_{\pi K^* K^*} \frac{f_{K^* N \Sigma^*}^{(1)}}{m_{K^*}} \mathcal{F}_t(q_V) \varepsilon^{\sigma\mu\alpha\beta} \frac{\mathcal{P}_{\beta\xi}}{t - m_{K^*}^2}$$

$$\gamma_{\eta} \gamma_5 [(k_1 - k_2)^{\nu} g^{\xi\eta} - (k_1 - k_2)^{\eta} g^{\xi\nu}]$$

$$k_{2\sigma} (k_1 - k_2)_{\alpha}, \quad (14)$$

$$\mathcal{A}_{u,(\Sigma)}^{\mu\nu} = -i\sqrt{2} g_{K^* N \Sigma} \frac{g_{\Sigma^* \pi \Sigma}}{m_{\pi}} \mathcal{F}_u(q_{\text{ex}}) k_1^{\nu} \frac{(q_{\Sigma} + m_{\Sigma})}{u - m_{\Sigma}^2}$$

$$\left(\gamma^{\mu} + \frac{\kappa_{K^* N \Sigma}}{4m_N} (\gamma^{\mu} \not{k}_2 - \not{k}_2 \gamma^{\mu}) \right), \quad (15)$$

with

$$\mathcal{P}^{\beta\xi} = i(g^{\beta\xi} + q_{K^*}^{\beta} q_{K^*}^{\xi} / m_{K^*}^2), \quad (16)$$

where $s = (k_1 + p_1)^2$, $t = (k_1 - k_2)^2$, and $u = (p_2 - k_1)^2$ are the Mandelstam variables.

2.2. Reggeized treatment

The Reggeized treatment is often used to analyze hadron production in the middle and high energy regions [21, 26, 28, 47, 51]. For the reaction $\pi^- p \rightarrow K^* \Sigma^*$, the energy range of the relevant experimental data is mainly concentrated in the middle energy zone, thus we will study this reaction channel in the Feynman model and the Regge model, respectively. Usually, it can be introduced by replacing the t -channel Feynman propagator in the Feynman amplitudes in equations (13) and (14) by the Regge propagator as [21, 26, 28, 47, 51],

$$\frac{1}{t - m_K^2} \rightarrow \left(\frac{s}{s_{\text{scale}}} \right)^{\alpha_K(t)} \frac{\pi \alpha'_K}{\Gamma[1 + \alpha_K(t)] \sin[\pi \alpha_K(t)]}, \quad (17)$$

$$\frac{1}{t - m_{K^*}^2} \rightarrow \left(\frac{s}{s_{\text{scale}}} \right)^{\alpha_{K^*}(t)-1} \frac{\pi \alpha'_{K^*}}{\Gamma[\alpha_{K^*}(t)] \sin[\pi \alpha_{K^*}(t)]}. \quad (18)$$

The scale factor s_{scale} is fixed at 1 GeV. Moreover, the meson Regge trajectories $\alpha_K(t)$ and $\alpha_{K^*}(t)$ are given by [26],

$$\alpha_K(t) = 0.70(t - m_K^2), \quad \alpha_{K^*}(t) = 1 + 0.85(t - m_{K^*}^2). \quad (19)$$

With the Regge model, no additional parameters are added. The only free parameter is the cutoff Λ , and its value needs to be discussed later in conjunction with the experimental data.

3. Numerical results

After the above preparation, one can calculate the differential cross-section of the $\pi^- p \rightarrow K^* \Sigma^*$ reaction and combine the experimental data [41–45] for correlation analysis. The differential cross-section in the center of mass (c.m.) frame is

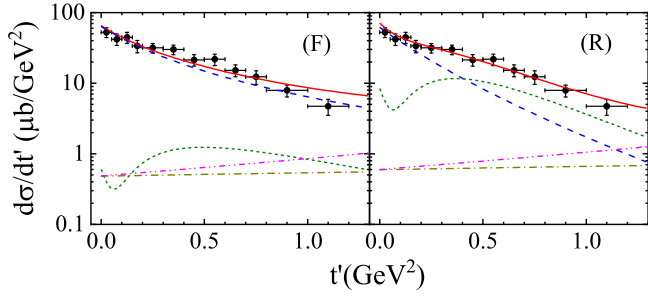


Figure 2. The t distribution for the reaction $\pi^-p \rightarrow K^*\Sigma^*$. The data are from [44]. The marks (F) and (R) are for the Feynman model and the Regge model, respectively. The full (red), dashed (blue), short-dashed (green), dashed-dotted (dark yellow) and dash-double dotted (magenta) lines are for the full model, K exchange, K^* exchange, s and u channel.

written as follows

$$\frac{d\sigma}{d\cos\theta} = \frac{1}{32\pi s} \frac{|\vec{k}_2^{\text{c.m.}}|}{|\vec{k}_1^{\text{c.m.}}|} \left(\frac{1}{2} \sum_{\lambda} |\mathcal{M}|^2 \right), \quad (20)$$

where $s = (k_1 + p_1)^2$, and θ denotes the angle of the outgoing K^* meson relative to the π beam direction in the c.m. frame. Here, $\vec{k}_1^{\text{c.m.}}$ and $\vec{k}_2^{\text{c.m.}}$ are the three-momenta of the initial π beam and final K^* , respectively.

3.1. Fitting procedure

With the help of the MINUIT code in the CERNLIB, the experimental data [41–45] of the $\pi^-p \rightarrow K^*\Sigma^*$ reaction will be fitted in two schemes: the Regge model and the Feynman model. As shown in figures 2–3, there are a total of 18 experimental data points for the reaction $\pi^-p \rightarrow K^*\Sigma^*$, including six total cross-section data and 12 data of the t distribution. Hence, one minimizes χ^2 per degree of freedom (d.o.f.) for the 18 data points by fitting three parameters, which include the coupling constant $f_{KN\Sigma^*}$ and the cutoffs Λ_t and Λ_u . As mentioned above, to minimize the free parameters, one sets $\Lambda_s = \Lambda_u$. The fitted values of the free parameters in two schemes are listed in table 1.

One notices that the values of the parameters fitted by the two models are close, except that the difference in the Λ_t value is relatively large. Moreover, the best-fitted χ^2 for the two schemes are 2.38 and 1.54 for the Feynman and the Regge models, respectively, which may mean that the Regge model is more consistent with the experimental data than the Feynman model. The best-fitted results given by the two schemes are presented in figures 2 and 3.

3.2. t distribution for reaction $\pi^-p \rightarrow K^*\Sigma^*$

The t distribution for the reaction $\pi^-p \rightarrow K^*\Sigma^*$ at $P_{\text{lab}} = 3.95$ GeV/c in two models is presented in figure 2. It is found that although both models can explain the experimental data well, the fitting of the data by the Regge model is significantly better than the fitting of the Feynman model to the experiment. In addition, we found that the contributions of the s and u channels are small in the results given by the two models, and the cross-section is basically derived from the

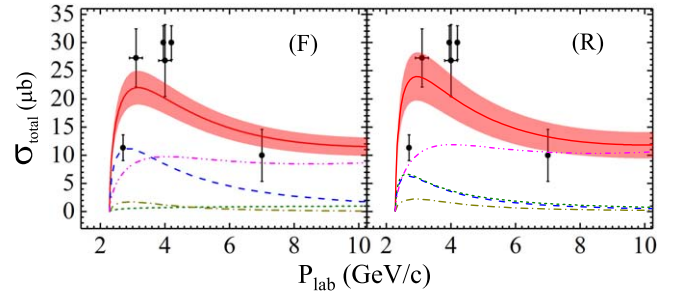


Figure 3. The total cross-section for the $\pi^-p \rightarrow K^*\Sigma^*$ reaction. The experimental data are from [41–45]. The notations are as in figure 2. The band stands for the error bars of the three fitting parameters in table 1. For the Feynman model, the error from the coupling constant $f_{KN\Sigma^*}$ accounts for about 30% of the error band width, while for the Regge model, the error from the coupling constant $f_{KN\Sigma^*}$ accounts for about 20% of the error band width.

Table 1. Fitted values of free parameters with all 18 data points in [41–45].

	Λ_t	$\Lambda_s = \Lambda_u$	$f_{KN\Sigma^*}$	χ^2/dof
Feynman	0.98 ± 0.01	0.75 ± 0.01	0.54 ± 0.02	2.38
Regge	1.67 ± 0.04	0.77 ± 0.02	0.55 ± 0.03	1.54

contribution of the t channel. In the Feynman model, the contribution of the t -channel K exchange is dominant, and the contribution from the t -channel K^* exchange is very small. However, in the Regge model, the contributions of the t -channel K and K^* exchanges are almost equivalent, and they each give their own contribution at different t .

3.3. Cross section of reaction $\pi^-p \rightarrow K^*\Sigma^*$

The total cross sections of the reaction $\pi^-p \rightarrow K^*\Sigma^*$ obtained in two schemes are illustrated in figure 3, which show that the contribution from the s channel is small, but the u channel plays a very important role, especially at higher energy. In both models, the contribution of the t channel is mainly concentrated at low energy, and the relative contributions of K and K^* exchanges are similar to that in figure 2. The contribution of the t channel exhibits the same pattern as the results in figure 2. That is, in the Feynman model, the contribution of the K exchange is much larger than the contribution of the K^* exchange, while in the Regge model, the contributions of the K exchange and the K^* exchange are comparable. Moreover, it is found that the total cross-section we obtained only reached the lower limit of the experimental data points at $P_{\text{lab}} = 3.1\text{--}4.2$ GeV/c, which may mean that there is also a contribution from s channel resonance in this region. When we consider the error bars of the fitting parameters, the total cross-section obtained will fit better with the data at $P_{\text{lab}} = 3.1\text{--}4.2$ GeV/c, but it still does not reach the highest point of the data. Since the data points of this energy region are very old at present, and there are few studies on the resonance state that can decay to $K^*\Sigma^*$, it is difficult to clarify the contribution of the resonance state of this energy region. Therefore, the measurement of experimental data with higher

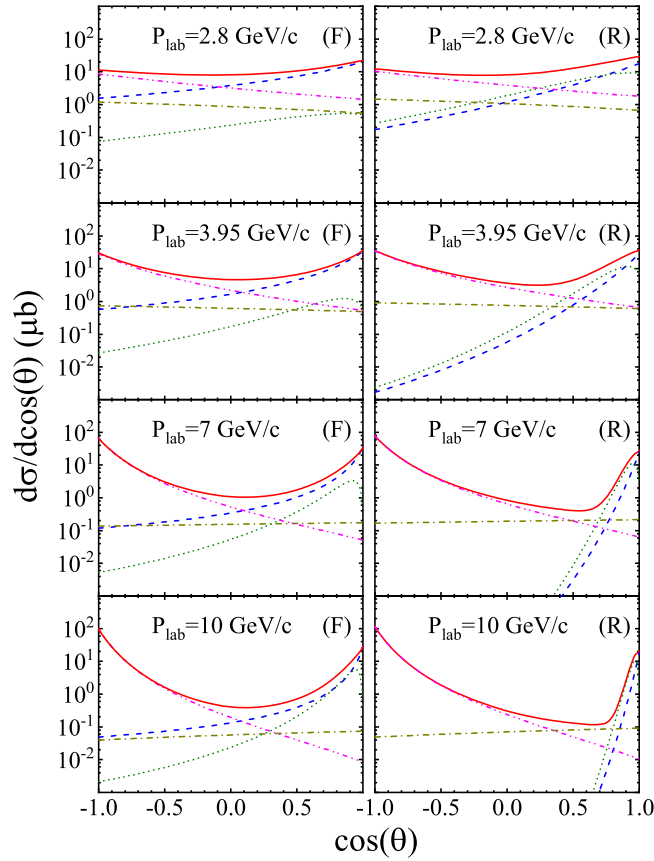


Figure 4. The differential cross-section $d\sigma/d\cos\theta$ for the $\pi^-p \rightarrow K^*\Sigma^*$ reaction as a function of $\cos\theta$. The notations are as in figure 2.

precision in this energy region and the theoretical prediction of the relevant resonance state are greatly needed.

The predictions of the differential cross-section of the reaction $\pi^-p \rightarrow K^*\Sigma^*$ in two schemes at different beam momenta are presented in figure 4, which shows that the discrepancy of the differential cross sections in the two models is small at low beam momenta but gradually increases in the higher beam momenta, especially in the forward angle region. Moreover, one notices that the contribution from the t channel is dominant at forward angles, while the contribution from the u channel becomes more and more important at backward angles with the increase in the energy. As in the previous case, the contribution of the s channel is small and negligible.

4. Summary and discussion

Within an effective Lagrangian approach, a three-parameter fitting is applied to the experimental data of the reaction $\pi^-p \rightarrow K^*\Sigma^*$ with the Feynman and Regge models, which leads to best-fitted values of χ^2 for the two schemes that are 2.38 and 1.54, respectively. For the t distribution for the reaction $\pi^-p \rightarrow K^*\Sigma^*$ at $P_{\text{lab}} = 3.95$ GeV/c, the fitting of the Regge model to the experimental data is better than the

Feynman model. But the quality of the fitting of the two models to the total cross-section data is similar.

From the fitting results, the contribution from the t channel is very large, the contribution of the s channel is small and negligible, and the contribution of the u channel is mainly concentrated in the high energy. The only difference is that the contributions of the t -channel K exchange and the K^* exchange are comparable in the Regge model, while in the Feynman model, the contribution of the K exchange is greater than that of the K^* exchange. In addition, the fitting results for the total cross-section seem to indicate a contribution from the s -channel resonance state at a center of mass energy of 2.6–2.97 GeV. Therefore, the $\pi^-p \rightarrow K^*\Sigma^*$ reaction may be an effective channel for finding the hidden strange pentaquark. More theoretical predictions about the resonance state that can decay to $K^*\Sigma^*$ are greatly needed for our subsequent research.

Finally, we also give the prediction of the differential cross-section of the $\pi^-p \rightarrow K^*\Sigma^*$ reaction at different beam momentum. The results show that the difference in the shape of the cross-section given by the two models increases with the increase in energy, especially in the forward angle region. This situation will help to clarify the role of the Regge propagator, and can be verified by future experiments.

The J-PARC, COMPASS, and JLAB are capable of producing high-intensity pion meson beams, which are expected to yield high-quality data for the $K^*\Sigma^*$ production. Our theoretical results will provide valuable information for such experiments. Combined with the corresponding photoproduction of $K^*\Sigma^*$ at JLAB 12 GeV upgraded, it is of great significance for a deeper understanding of the relevant reaction mechanism and the search for the hidden strange pentaquark.

Acknowledgments

X-Y W would like to acknowledge Dr Quanjin Wang for useful discussions. We acknowledge the National Natural Science Foundation of China under Grant No. 11705076 and No. 11675228. This work is partly supported by the HongLiu Support Funds for Excellent Youth Talents of Lanzhou University of Technology. This work is also supported by the Fundamental Research Funds for the Central Universities.

References

- [1] Tanabashi M *et al* (Particle Data Group) 2018 Review of particle physics *Phys. Rev. D* **98** 030001
- [2] Capstick S and Roberts W 2000 Quark models of baryon masses and decays *Prog. Part. Nucl. Phys.* **45** S241
- [3] Nerling F and (COMPASS Collaboration) 2012 Hadron spectroscopy with COMPASS: newest results *EPJ Web Conf.* **37** 01016
- [4] Kumano S 2016 Spin physics at J-PARC *Int. J. Mod. Phys. Conf. Ser.* **40** 1660009
- [5] Capstick S and Roberts W 1998 Strange decays of nonstrange baryons *Phys. Rev. D* **58** 074011
- [6] Capstick S and Roberts W 1994 Quasi two-body decays of nonstrange baryons *Phys. Rev. D* **49** 4570

- [7] Zou B S and Riska D O 2005 The s anti-s component of the proton and the strangeness magnetic moment *Phys. Rev. Lett.* **95** 072001
- [8] Liu B C and Zou B S 2006 Mass and K Lambda coupling of $N^*(1535)$ *Phys. Rev. Lett.* **96** 042002
- [9] Wu J J, Molina R, Oset E and Zou B S 2010 Prediction of narrow N^* and Λ^* resonances with hidden charm above 4 GeV *Phys. Rev. Lett.* **105** 232001
- [10] Yuan S G, Wei K W, He J, Xu H S and Zou B S 2012 Study of $qqqc\bar{c}$ five quark system with three kinds of quark-quark hyperfine interaction *Eur. Phys. J. A* **48** 61
- [11] Yang Z C, Sun Z F, He J, Liu X and Zhu S L 2012 The possible hidden-charm molecular baryons composed of anti-charmed meson and charmed baryon *Chin. Phys. C* **36** 6
- [12] Aaij R et al (LHCb Collaboration) 2019 Observation of a narrow pentaquark state, $P_c(4312)^+$, and of two-peak structure of the $P_c(4450)^+$ *Phys. Rev. Lett.* **122** 222001
- [13] Aaij R et al (LHCb Collaboration) 2015 Observation of $J/\psi p$ resonances consistent with pentaquark states in $\Lambda_b^0 \rightarrow J/\psi K^- p$ decays *Phys. Rev. Lett.* **115** 072001
- [14] He J 2017 Nucleon resonances $N(1875)$ and $N(2100)$ as strange partners of LHCb pentaquarks *Phys. Rev. D* **95** 074031
- [15] Wang X Y, He J, Chen X R, Wang Q and Zhu X 2019 Pion-induced production of hidden-charm pentaquarks $P_c(4312)$, $P_c(4440)$, and $P_c(4457)$ *Phys. Lett. B* **797** 134862
- [16] Wang X Y, He J and Chen X 2020 Systematic study of the production of hidden-bottom pentaquarks via γp and $\pi^- p$ scatterings *Phys. Rev. D* **101** 034032
- [17] Xie J J and Nieves J 2010 The role of the $N^*(2080)$ resonance in the $\bar{\gamma} p \rightarrow K^+ \Lambda(1520)$ reaction *Phys. Rev. C* **82** 045205
- [18] He J 2014 Theoretical study of the $\Lambda(1520)$ photoproduction off proton target based on the new CLAS data *Nucl. Phys. A* **927** 24
- [19] He J and Chen X R 2012 The roles of nucleon resonances in $\Lambda(1520)$ photoproduction off proton *Phys. Rev. C* **86** 035204
- [20] He J 2014 $\Sigma(1385)$ photoproduction from proton within a Regge-plus-resonance approach *Phys. Rev. C* **89** 055204
- [21] Wang X Y, He J and Haberzettl H 2016 Analysis of recent CLAS data on $\Sigma^*(1385)$ photoproduction off a neutron target *Phys. Rev. C* **93** 045204
- [22] Yu B G and Kong K J 2017 Photoproduction of $\gamma N \rightarrow K^+ \Sigma^*(1385)$ in the Reggeized framework *Phys. Rev. C* **95** 065210
- [23] Yu B G and Kong K J 2017 Photoproduction of $\gamma p \rightarrow K^+ \Lambda^*(1520)$ and decay of $\Lambda^*(1520) \rightarrow K^- p$ in the Reggeized framework *Phys. Rev. C* **96** 025208
- [24] He J 2015 Internal structures of the nucleon resonances $N(1875)$ and $N(2120)$ *Phys. Rev. C* **91** 018201
- [25] Oh Y and Kim H 2006 K^* photoproduction off the nucleon: $\gamma n \rightarrow K^* \Lambda$ *Phys. Rev. C* **73** 065202
- [26] Ozaki S, Nagahiro H and Hosaka A 2010 Charged K^* photoproduction in a Regge model *Phys. Rev. C* **81** 035206
- [27] Kim S H, Nam S I, Oh Y and Kim H C 2011 Contribution of higher nucleon resonances to $K^* \Lambda$ photoproduction *Phys. Rev. D* **84** 114023
- [28] Wang X Y and He J 2016 $K^{*0} \Lambda$ photoproduction off a neutron *Phys. Rev. C* **93** 035202
- [29] Yu B G, Oh Y and Kong K J 2017 Regge approach to the reaction of $\gamma N \rightarrow K^* \Lambda$ *Phys. Rev. D* **95** 074034
- [30] Oh Y, Ko C M and Nakayama K 2008 Nucleon and Delta resonances in K Sigma(1385) photoproduction from nucleons *Phys. Rev. C* **77** 045204
- [31] Nam S I, Hosaka A and Kim H C 2005 $\Lambda(1520, 3/2^-)$ photoproduction reaction via $\gamma N \rightarrow K \Lambda(1520)$ *Phys. Rev. D* **71** 114012
- [32] Nam S I and Kao C W 2010 $\Lambda(1520)$ photoproduction off the proton target with Regge contributions *Phys. Rev. C* **81** 055206
- [33] Nakayama K, Oh Y and Haberzettl H 2006 Photoproduction of Ξ off nucleons *Phys. Rev. C* **74** 035205
- [34] Borekov K G and Kaidalov A B 1983 Production of charmed baryons in hadron hadron collisions *Sov. J. Nucl. Phys.* **37** 100
- [35] Borekov K G and Kaidalov A B 1983 Production of charmed baryons in hadron hadron collisions *Yad. Fiz.* **37** 174
- [36] Grishina V Y, Kondratyuk L A, Cassing W, Mirazita M and Rossi P 2005 Comparative Regge analysis of Λ , $\Sigma \Lambda(1520)$ and Θ^+ production in γp , πp and pp reactions *Eur. Phys. J. A* **25** 141
- [37] Kim S H, Hosaka A, Kim H C and Noumi H 2015 Production of strange and charmed baryons in pion induced reactions *Phys. Rev. D* **92** 094021
- [38] Kim S H, Oh Y and Titov A I 2017 Decay angular distributions of K^* and D^* vector mesons in pion-nucleon scattering *Phys. Rev. C* **95** 055206
- [39] Kim S H, Kim H C and Hosaka A 2016 $K^0 \Lambda$ and $D^- \Lambda_c^+$ production induced by pion beams off the nucleon *Phys. Rev. D* **94** 094025
- [40] Wang X Y and He J 2019 Production of $\phi(2170)$ and $\eta(2225)$ in a kaon induced reaction *Eur. Phys. J. A* **55** 152
- [41] Dahl O I, Hardy L M, Hess R I, Kirz J and Miller D H 1967 Strange-particle production in $\pi^- p$ interactions from 1.5 to 4.2 BeV/c: I. Three-and-more-body final states *Phys. Rev.* **163** 1377
- [42] Miller D H, Kovacs A Z, McIlwain R, Palfrey T R and Tauffest G W 1965 Strange-particle production in 2.7-GeV/c $\pi^- p$ interactions *Phys. Rev.* **140** B360
- [43] Aguilar-Benitez M et al (CERN-College de France-Madrid-Stockholm Collaboration) 1980 Study of the reactions $\pi^- p \rightarrow K^0(890) \Lambda$, $K^0(890) \Sigma^0$ and $K^0(890) \Sigma^0(1385)$ at 3.95-GeV/c *Z. Phys. C* **6** 195
- [44] Aguilar-Benitez M et al (CERN-College de France-Madrid-Stockholm Collaboration) 1981 Study of the reactions $\pi^- p \rightarrow K^0(890) \Lambda$, $K^0(890) \Sigma^0$ and $K^0(890) \Sigma^0(1385)$ at 3.95-GeV/c *Z. Phys. C* **8** 188 Erratum:
- [45] Aguilar-Benitez M and Irving A C 1981 The amplitude structure of the processes $K^- p \rightarrow \rho^- \Sigma^+(1385)$ and $K^- p \rightarrow \phi \Sigma^0(1385)$ at 4.2-GeV/c *Z. Phys. C* **11** 223
- [46] Peekna A, Walker W D, Oh B Y, Thompson M A, Clear D R, Hoa D N and Prentice J 1971 Strange-particle production in 7 GeV/c $\pi^- p$ interactions *Nucl. Phys. B* **27** 605
- [47] Xie J J and Zou B S 2007 The role of $\Delta^{++}(1620)$ resonances in $pp \rightarrow n K^+ \Sigma^+$ reaction and its important implications *Phys. Lett. B* **649** 405
- [48] Wang X Y and He J 2017 Investigation of pion-induced $f_1(1285)$ production off a nucleon target within an interpolating Reggeized approach *Phys. Rev. D* **96** 034017
- [49] Bando M, Kugo T and Yamawaki K 1988 Nonlinear realization and hidden local symmetries *Phys. Rep.* **164** 217
- [50] Oh Y and Kim H 2006 Scalar kappa meson in K^* photoproduction *Phys. Rev. C* **74** 015208
- [51] Wang X Y, Chen X R and He J 2019 Possibility to study pentaquark states $P_c(4312)$, $P_c(4440)$, and $P_c(4457)$ in $\gamma p \rightarrow J/\psi p$ reaction *Phys. Rev. D* **99** 114007
- [52] Storow J K 1984 Baryon exchange processes *Phys. Rep.* **103** 317